

Electronic Reconstruction in Correlated Electron Heterostructures:

Towards a general understanding of correlated electrons
at interface and surface

Satoshi Okamoto

Department of Physics, Columbia University

Collaborator: Andrew J. Millis

Support: JSPS & DOE ER 46169

Discussion: H.Monien, M.Potthoff, G.Kotliar, A.Ohtomo, H.Hwang

Journal Refs.:

S.O. & A.J.M., Nature **428**, 630 (2004); PRB **70**, 075101; 241104(R) (2004).

Interface Science including Correlated-Electron Systems

(ex. High- T_c cuprates, CMR manganites...)

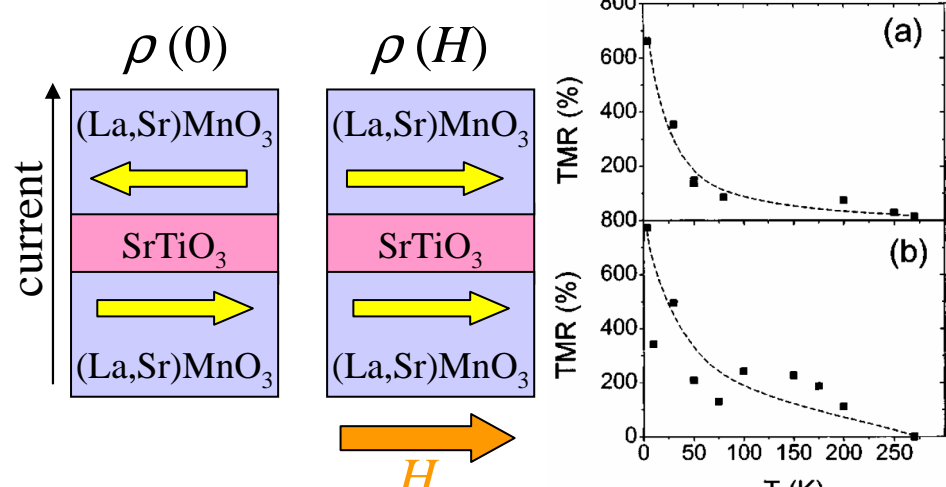
Important for Application: spin valve, Josephson junction...

Experiment (surface* sensitive): ARPES, STM,...

*Surface= interface between material & vacuum

Tunneling magnetoresistance (TMR)
 $(\text{La},\text{Sr})\text{MnO}_3/\text{SrTiO}_3/(\text{La},\text{Sr})\text{MnO}_3$

Bowen *et al.*, Appl. Phys. Lett. **82**, 233 (2003).



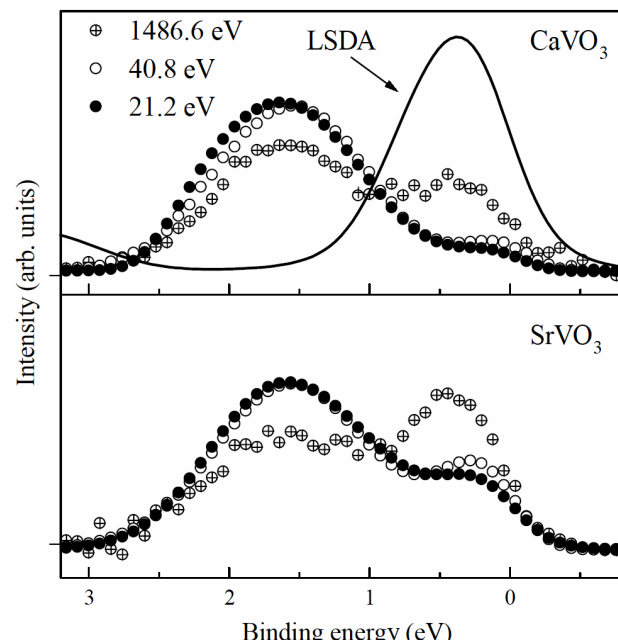
$$\text{TMR} = \frac{\rho(0) - \rho(H)}{\rho(H)} \xrightarrow[H \rightarrow \infty]{} \frac{2P^2}{1 - P^2}$$

High TMR ratio (high polarization $P \sim 90\%$)
 is only achieved at very low $T \ll \text{bulk } T_C \sim 370\text{K}$

Interface phases look different from bulk...

Photoemission experiment on CaVO_3 and SrVO_3

Maiti *et al.*, Europhys. Lett. **55**, 246 (2001).

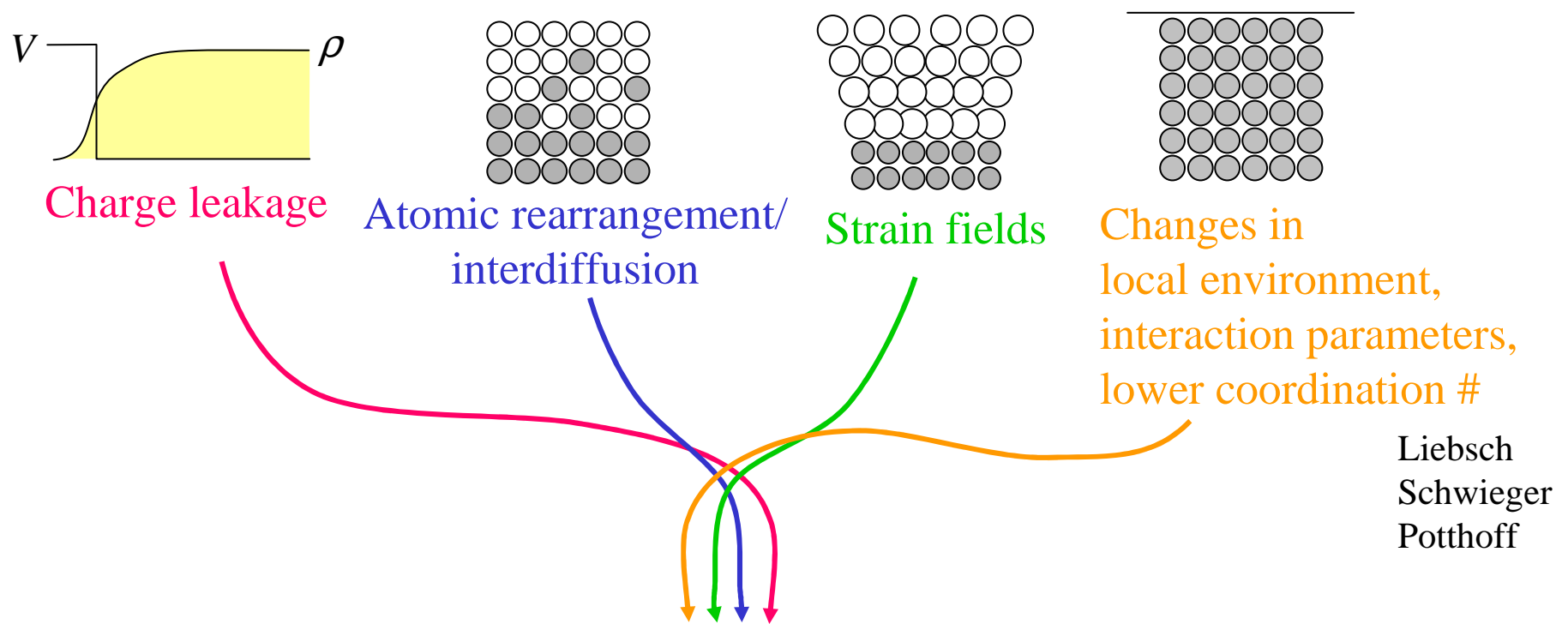


Dependent on photon energy
 Surface \neq bulk

Theory: Liebsch
 Schwieger, Potthoff

Key question: **What is electronic phase?** FM/AFM/SC, Metal/insulator,...
(contrast: usual surface science; what is lattice reconstruction)

What are important effects?



In this talk: Focus on
“Charge leakage”, “Magnetic ordering”, “Metal/insulator”

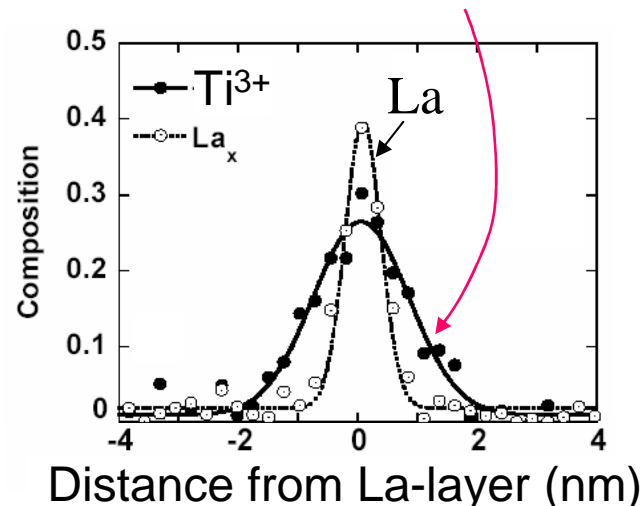
$[\text{LaTiO}_3]_n/[\text{SrTiO}_3]_m$ heterostructure

Ohtomo, Muller, Grazul, and Hwang, Nature **419**, 378 (2002)

Bulk: LaTiO_3 : Mott insulator with d^1
 SrTiO_3 : band insulator with d^0

EELS results of “1 La-layer” heterostructure

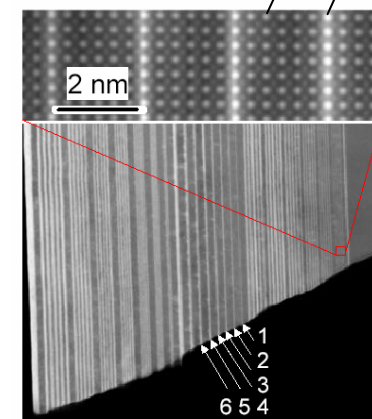
Fraction of Ti^{3+} : **d -electron density**



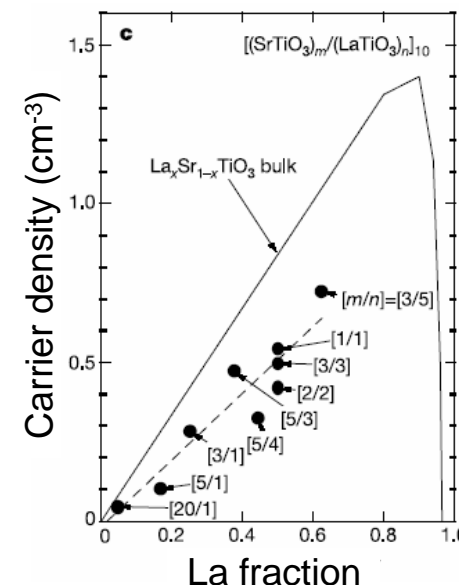
Substantial Charge leakage

Decay length $\sim 1\text{nm}$ (2~3 unit cells)

Dark field image Sr La



Transport property



**Heterostructure
is Metallic!!**

LaTiO_3 & SrTiO_3 have “almost the same lattice constant”
Ideal playground and good starting point!

This talk:

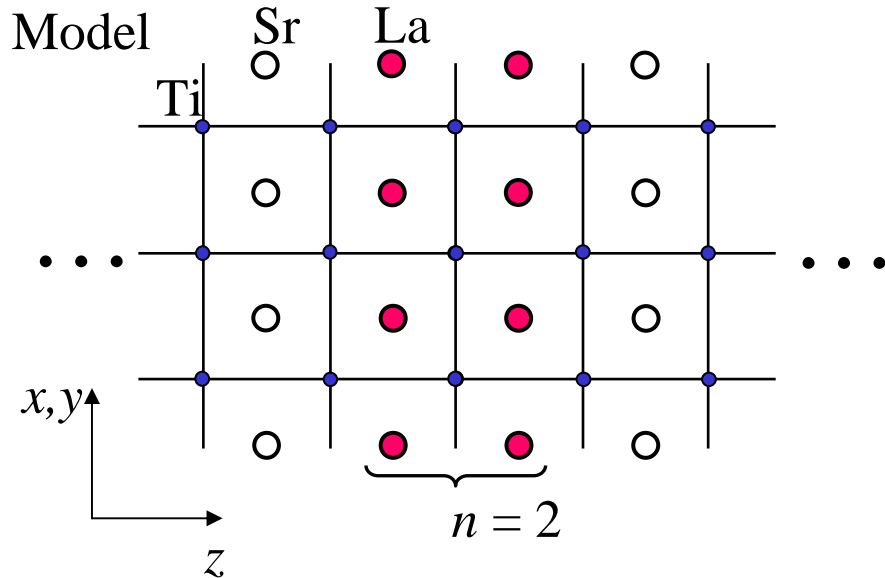
1. Realistic model calculation for $[\text{LaTiO}_3]_n/[\text{SrTiO}_3]_m$ -type heterostructure (“Ohtomo-structure”) based on **Hartree-Fock**
2. Beyond Hartree-Fock effect by **Dynamical-mean-field theory** using simplified model heterostructure
 - 2.1. Metallic interface and quasiparticle
 - 2.2. Magnetic ordering (on-going work)

Key word of theoretical results: “Electronic reconstruction”

- “Spin & Orbital orderings” in Heterostructures differ from bulk orderings
 - “Edge” region ~ 3 unit-cell wide — Metallic!!
- *Independent of detail of theory***

1. Realistic model calculation for $[\text{LaTiO}_3]_n/[\text{SrTiO}_3]_m$ -type heterostructure (“Ohtomo-structure”)

“Ohtomo-structure”



Ti d -electron (electronically active)

- tight-binding t_{2g} (xy , xz , yz) bands
- Strong on-site interaction
- Long-range repulsion

Extra “+1 charge” on La site (La^{3+} vs Sr^{2+})

- Potential for d -electron

Neutrality condition

- # of Ti d -electron = # of La ion

Self-consistent screening

Hamiltonian for Ti t_{2g} electron

$$t_{2g} \text{ bands } H_{hop}^{(a)} = \sum_{\langle ij \rangle, a, \sigma} [t_{ij}^a d_{ia\sigma}^\dagger d_{ja\sigma} + H.c.]$$

$t \sim 0.3 \text{ eV}$ Kimura *et al.* PRB **51**, 11049 (1995)

On-site Coulomb

$$H_{on-site}^{(i)} = U \sum_a n_{a\uparrow} n_{a\downarrow} + (U' - J) \sum_{a>b, \sigma} n_{a\sigma} n_{b\sigma} \\ + U' \sum_{a \neq b} n_{a\uparrow} n_{b\downarrow} + J \sum_{a \neq b} d_{a\uparrow}^\dagger d_{b\uparrow} d_{b\downarrow}^\dagger d_{a\downarrow}$$

U from ~2
to ~6 eV Okimoto *et al.*, PRB **51**, 9581 (1995)
Mizokawa & Fujimori, PRB **51**, 12880 (1995)

Electrostatic potential

$$H_{Coul}^{(i)} = V^{(i)} n_i \\ V^{(i)} = - \sum_{\text{La site}} \frac{e^2}{\epsilon |R_j^{La} - R_i|} + \frac{1}{2} \sum_{j \neq i} \frac{e^2 n_j}{\epsilon |R_j - R_i|}$$

Attraction by d - d repulsion
La ions

SrTiO_3 : Almost ferroelectric

$$\epsilon(q \rightarrow 0, T \rightarrow 0) \gg 10^2$$

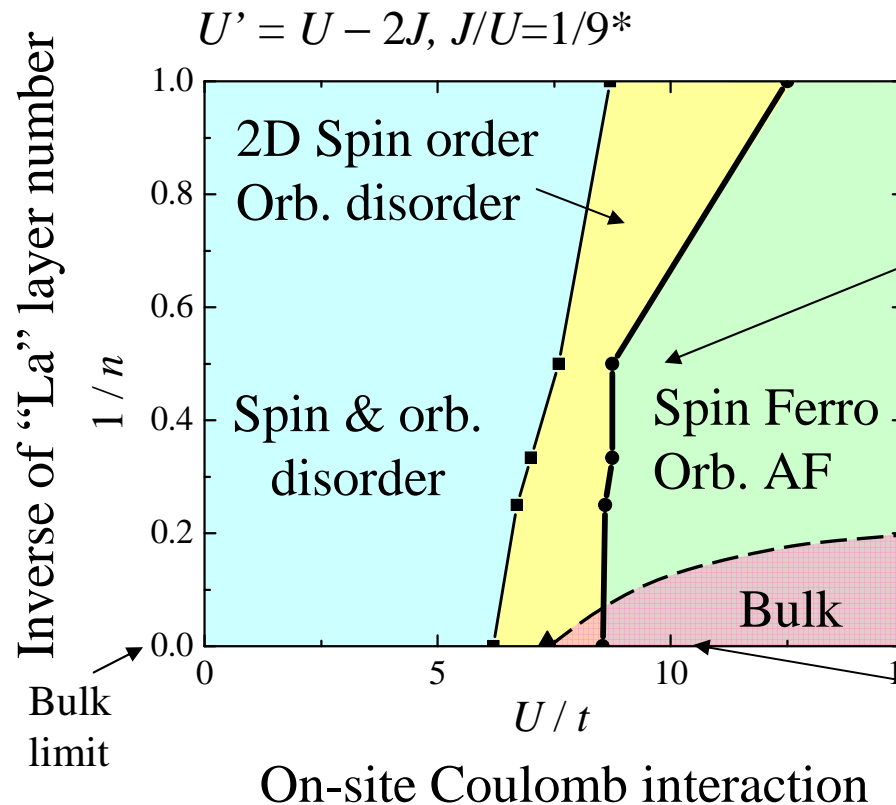
We need $\epsilon(l \sim 1\text{\AA}, T \sim 300\text{K})$

This work: $\epsilon = 15$

(Results do not change: $5 < \epsilon < 40$)

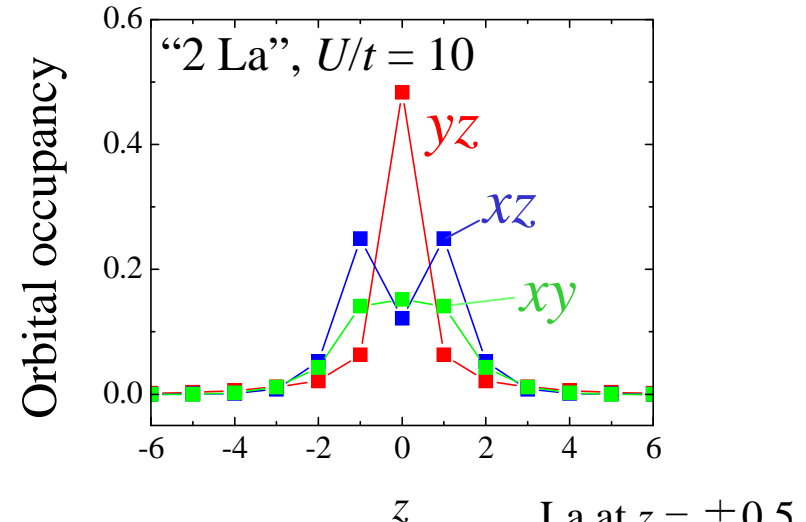
Key point: Different Spin & Orbital orderings than in the bulk “Electronic reconstruction”

Hartree-Fock result for
the Ground-state phase diagram

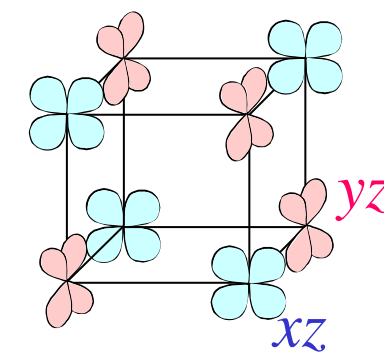


Details of phase diagram may depend on approximation method.

Difference from bulk — generic



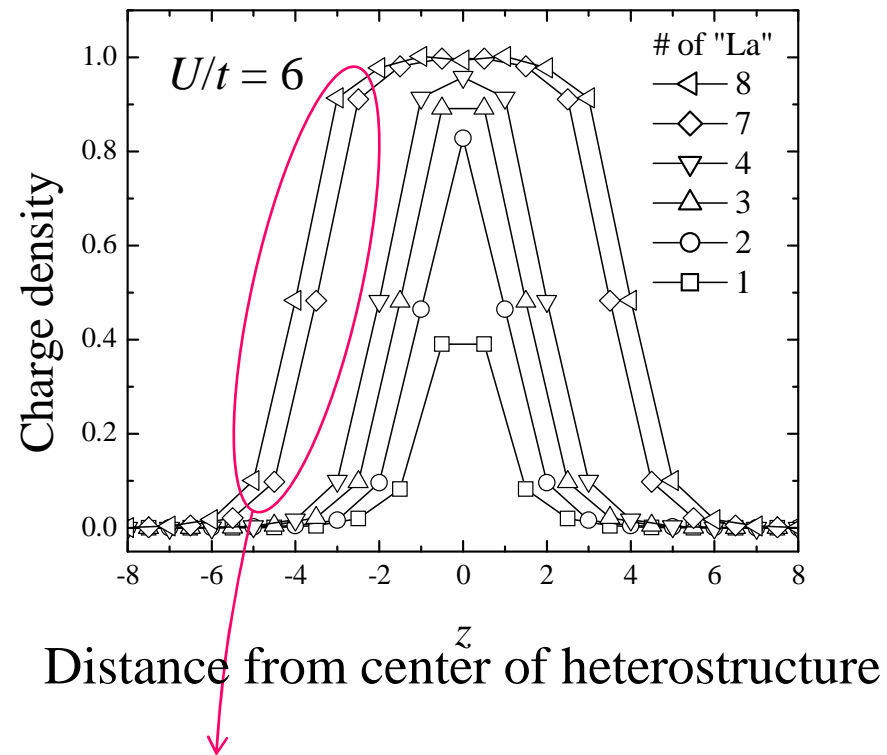
2-dimensional orbital order
(in-plane-translational symmetry)



Bulk: 3D AF orbital

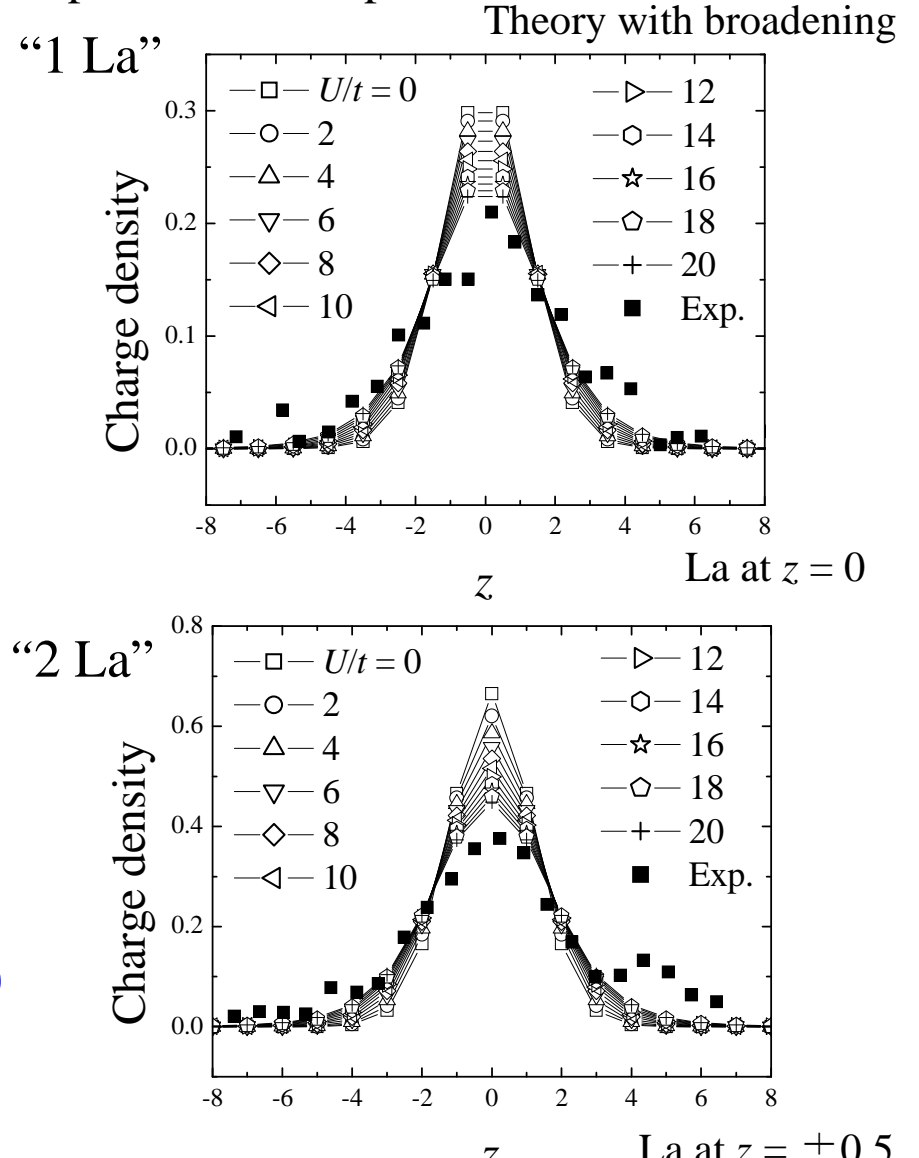
* Similar ratio is reported by photoemission

Spatial charge distribution



Bulk like property at the center site
at # of La (n) > 6
Compatible with the experiment?
—mainly $n < 6$ studied.

Comparison with experiments

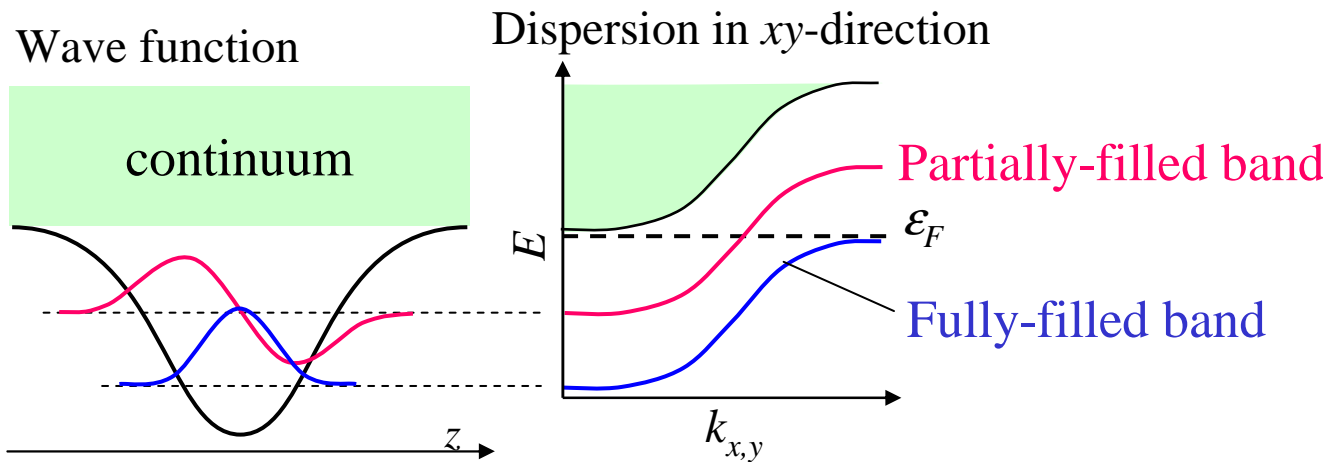


Charge distribution width
(Theory) \gtrsim (experiments)

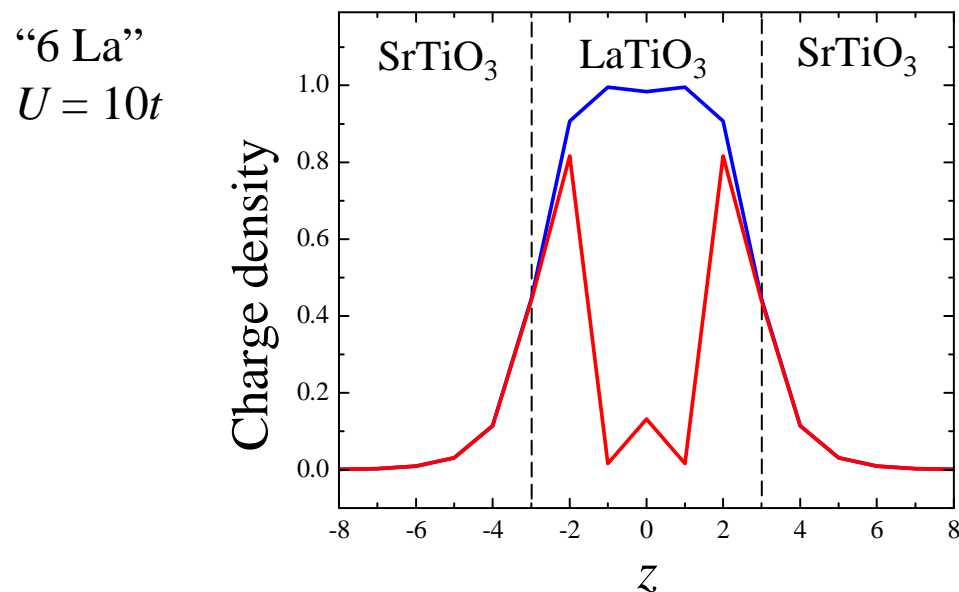
Sub-band structure and metallicity

Hartree-Fock picture

Schematic view of sub-band structure



Total electron density (blue) and
electron density from the partially-filled bands (red)

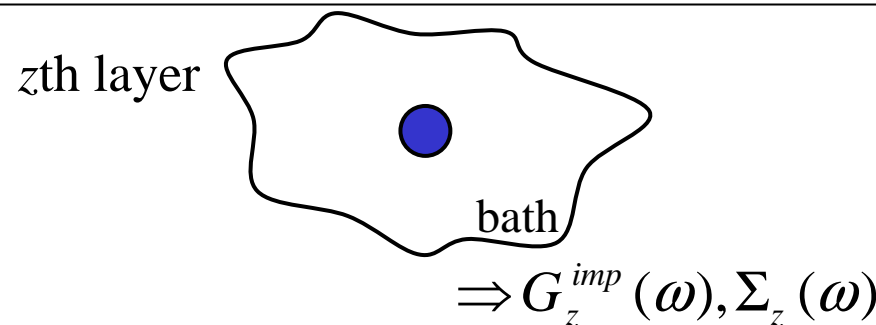
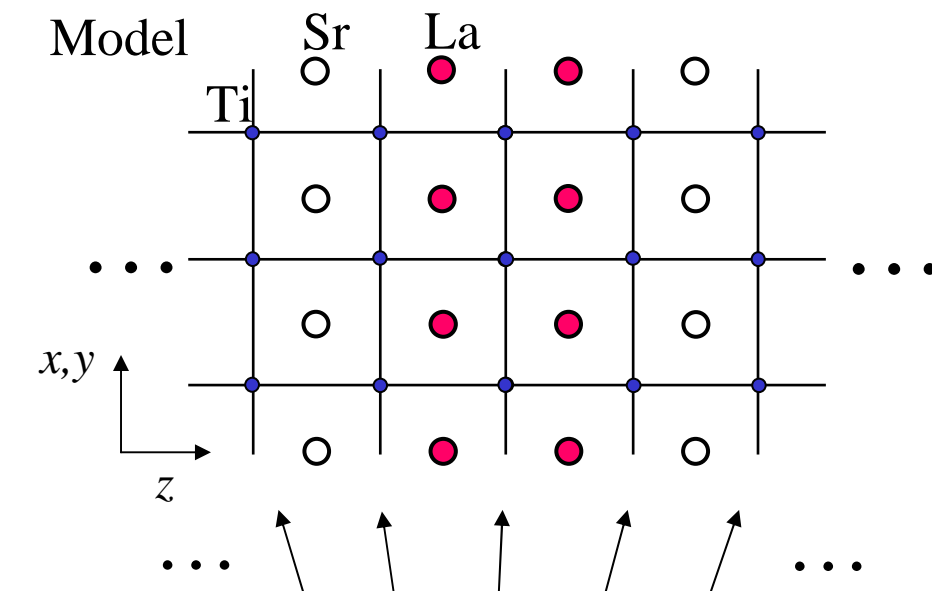


“Edge region” is metallic!!

Another example of
“Electronic reconstruction”

- 2. Beyond Hartree-Fock by **Dynamical-mean-field theory (DMFT)**
 - 2.1. Metallic interface and quasiparticle
 - 2.2. Magnetic ordering (on-going work)

Beyond Hartree-Fock effects by **Dynamical-mean-field theory (DMFT)**



Remaining problem:
Solving many impurity models is computationally expensive.
We need to solve many impurities.

Single-band heterostructure

$$H = H_{hop} + \sum_i [H_{on-site}^{(i)} + H_{Coul}^{(i)}]$$

$$H_{hop} = -t \sum_{\langle ij \rangle \sigma} [d_{i\sigma}^\dagger d_{j\sigma} + H.c.]$$

$$H_{on-site}^{(i)} = U n_{i\uparrow} n_{i\downarrow} \Leftarrow \text{Single-band Hubbard}$$

$$H_{Coul}^{(i)} = V^{(i)} n_i \quad V^{(i)} = - \sum_j \frac{e^2}{\epsilon |R_j^{La} - R_i|} + \frac{1}{2} \sum_{j \neq i} \frac{e^2 n_j}{\epsilon |R_j - R_i|}$$

Key assumption for DMFT:

Self-energy $\Sigma_{zz}(k_{||}, \omega)$ is layer-diagonal and independent of in-plane momentum $k_{||}$

Self-consistency

$$G_z^{imp}(\omega) = \int \frac{d^2 k_{||}}{(2\pi)^2} G_{zz}^{latt}(k_{||}, \omega)$$

$$\hat{G}_{zz}^{latt}(k_{||}, \omega) = [\omega + \mu - \hat{H}_0(k_{||}) - \hat{\Sigma}(\omega)]^{-1}$$

$$\hat{H}_0 : H_{hop} + H_{Coul}^{Hartree} \quad \Sigma_{zz}(\omega) = \Sigma_z(\omega) \delta_{zz}$$

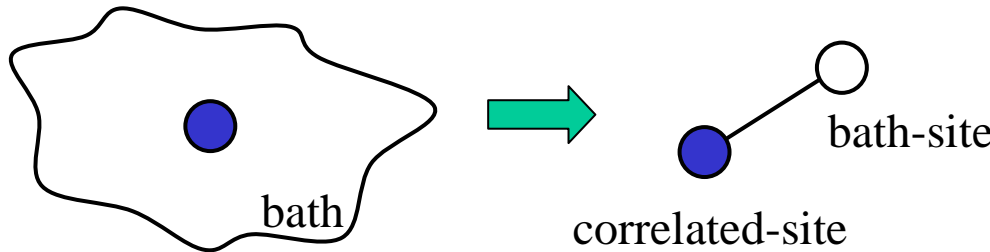
+ self-consistency for charge distribution

DMFT study 1: “Metallic interface” and quasiparticle band

We need impurity solver which becomes reasonable at high- and low-frequency regions

2-site DMFT

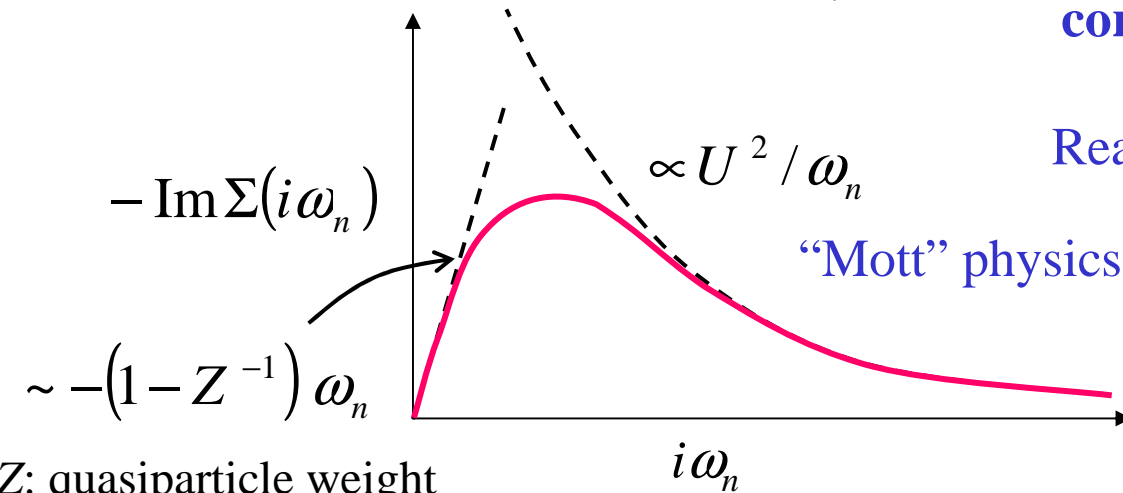
Potthoff, PRB, 64, 165114 (2001)



Self-energy

$$\Sigma(i\omega_n) = \alpha_0 + \frac{\alpha_1}{i\omega_n - \omega_1} + \frac{\alpha_2}{i\omega_n - \omega_2}$$

Schematic view of “correct” $\Sigma(i\omega_n)$



Z: quasiparticle weight

Mass enhancement

2-site DMFT self-energy has correct behavior at two limits

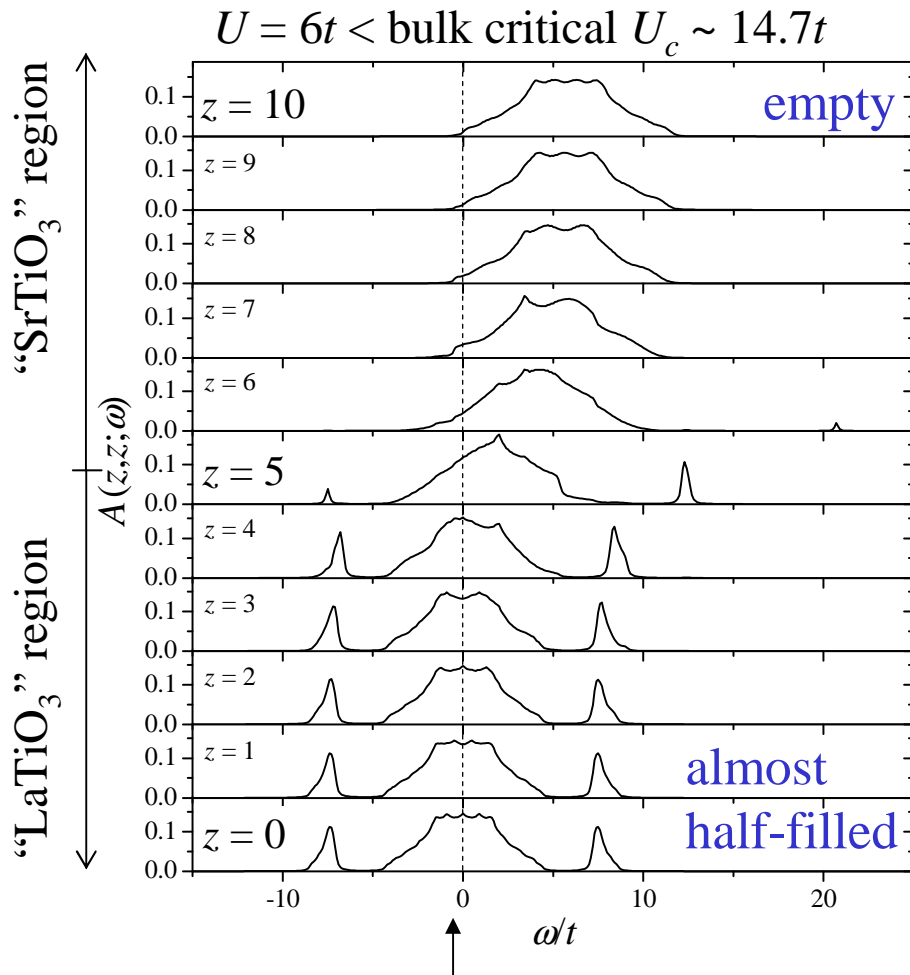
$\omega \rightarrow 0$ & $\omega \rightarrow \infty$

Reasonable behavior in between

Results: Layer resolved spectral function $A(z,z;\omega) = -\frac{1}{\pi} \text{Im} G_{zz}^{\text{latt}}(\omega)$

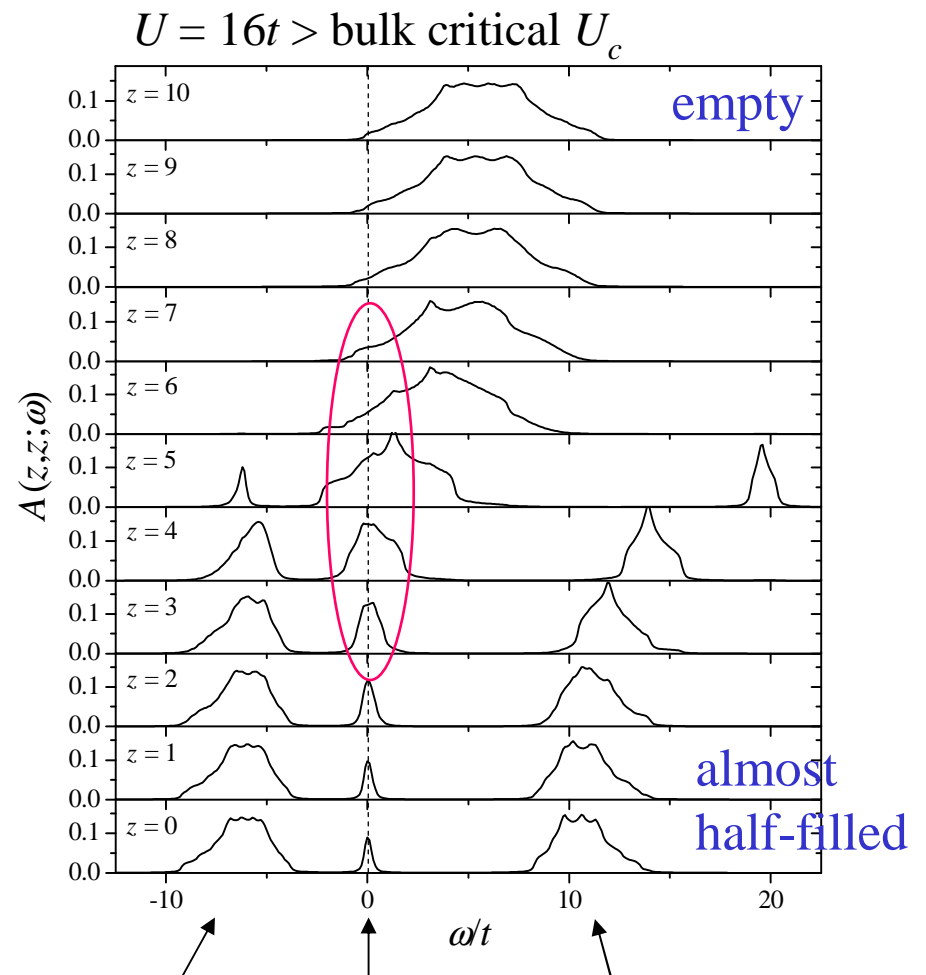
“10 La-layers” heterostructure (La at $z=-4.5, \dots, +4.5$)

Weak coupling regime



coherent quasiparticle-band
dominates the spectral weight

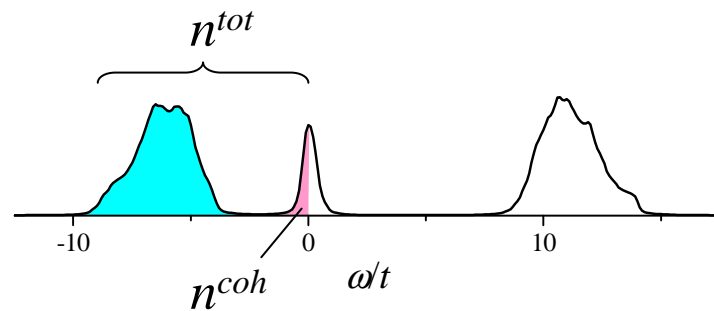
Strong coupling regime



Charge density distribution: “Visualization of metallic region”

n^{tot} : total charge density = $2 \int_{-\infty}^0 d\omega A(z, z; \omega)$

n^{coh} : quasiparticle (coherent) density = $2 \int_0^\infty d\omega A^{coh}(z, z; \omega)$

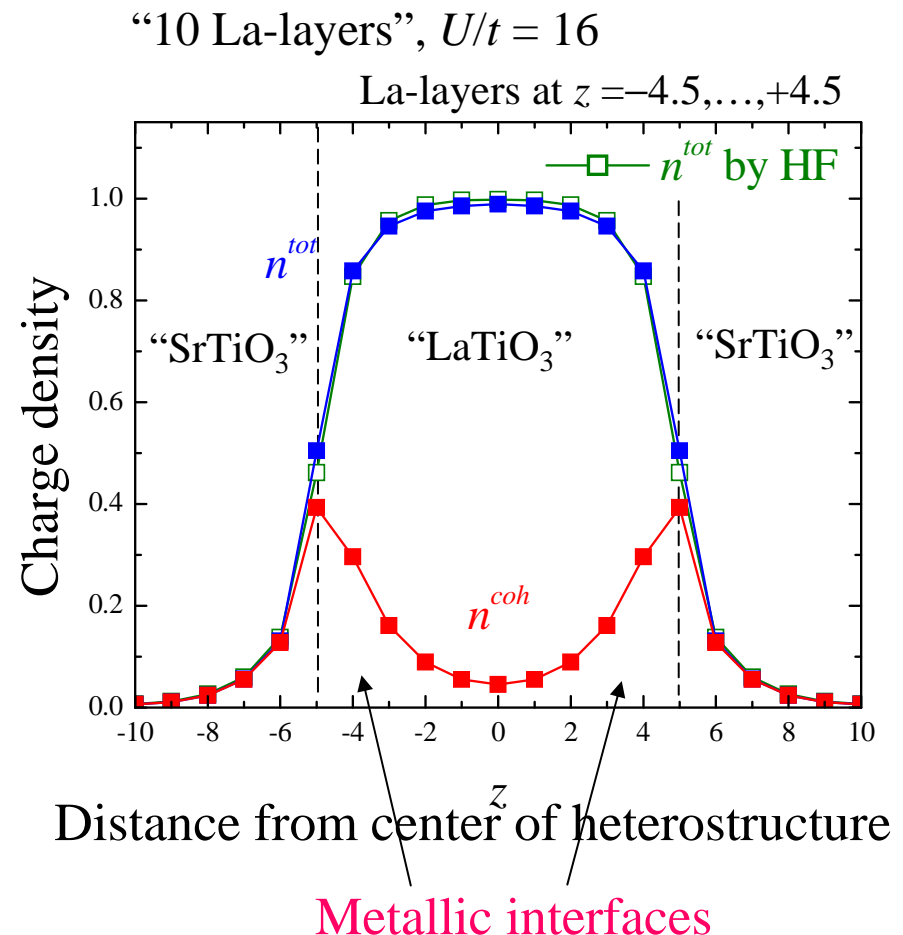


Center region is dominated by lower Hubbard band: insulating

Edge region, ~ 3 unit cell wide, is dominated by coherent quasiparticle: Metallic!!

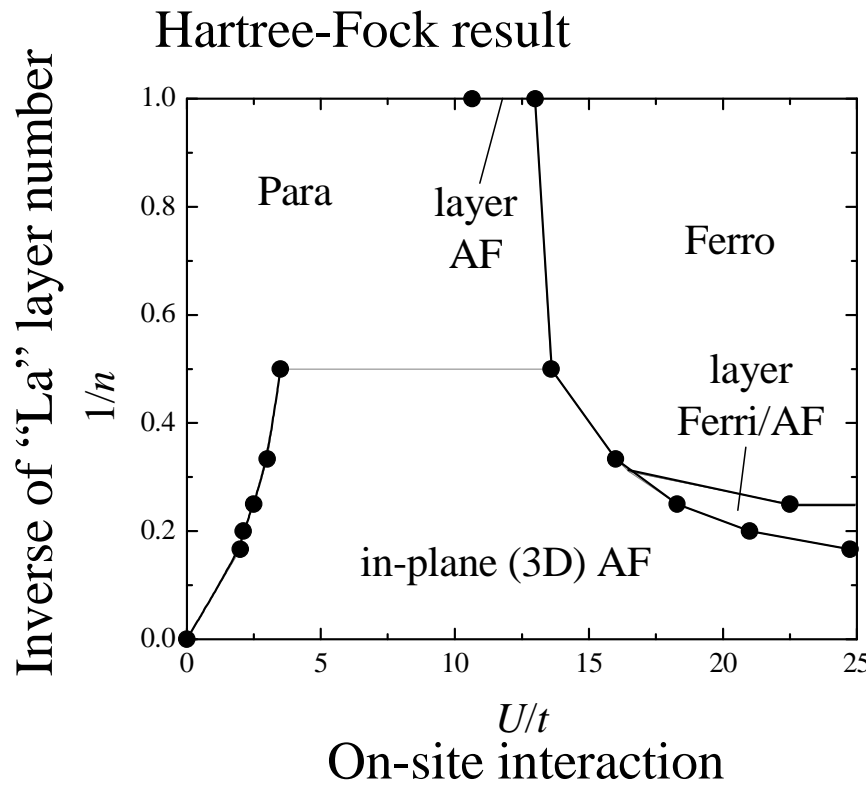
$n \gtrsim 6$ needed for “insulating” central Layers

DMFT & Hartree-Fock give almost identical charge distribution



DMFT study 2: Magnetic ordering

Magnetic Phase Diagram for 1-orbital model



Thin heterostructures show different magnetic orderings than in the bulk.
Ferromagnetic and layer Ferri/AF (in-plane translation symmetry) orderings at large U and small n region.

How is this phase diagram modified by beyond-Hartree-Fock effect?

How difficult is dealing with in-plane symmetry breaking?

DMFT Self-consistency equations

Without in-plane symmetry breaking

$$G_z^{imp}(\omega) = \int \frac{d^2 k_{\parallel}}{(2\pi)^2} G_{zz}^{latt}(k_{\parallel}, \omega)$$

$$\hat{G}_{zz'}^{latt}(k_{\parallel}, \omega) = \begin{bmatrix} \alpha_1 & t & & & \\ t & \alpha_2 & t & & \\ & t & \ddots & & \\ & & \ddots & t & \\ & & & t & \alpha_N \end{bmatrix}^{-1}$$

$$a_z = \omega + \mu - \varepsilon_{k\parallel} - V_z - \Sigma_z(\omega)$$

$\varepsilon_{k\parallel}$: in-plane dispersion

V_z : potential from long-ranged Coulomb

N : total layer #

With in-plane symmetry breaking

$$G_{zA(B)}^{imp}(\omega) = \int \frac{d^2 k_{\parallel}}{(2\pi)^2} G_{zA(B), zA(B)}^{latt}(k_{\parallel}, \omega)$$

$$\hat{G}_{zz'}^{latt}(k_{\parallel}, \omega) = \begin{bmatrix} \alpha_{1A} & t & & & & & & \\ t & \alpha_{2A} & t & & & & & \\ & t & \ddots & t & & & & \\ & & & t & \alpha_{NA} & & & \\ -\varepsilon_{k\parallel} & & & & & \alpha_{1B} & t & \\ & -\varepsilon_{k\parallel} & & & & t & \alpha_{2B} & t \\ & & \ddots & & & t & \ddots & t \\ & & & -\varepsilon_{k\parallel} & & & t & \alpha_{NB} \end{bmatrix}^{-1}$$

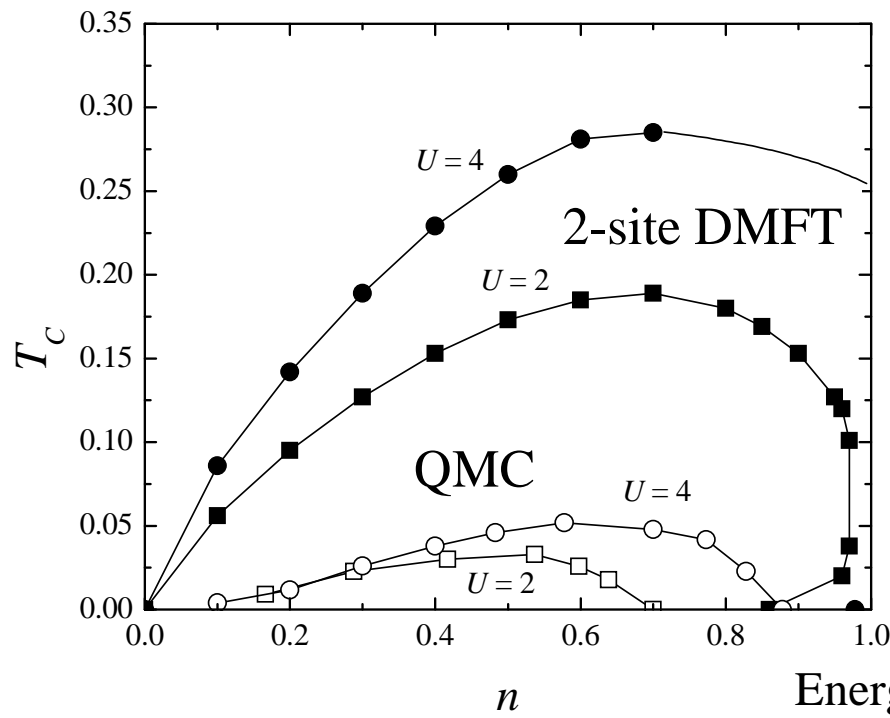
$$a_{zA(B)} = \omega + \mu - V_z - \Sigma_{zA(B)}(\omega)$$

We have to invert at least twice larger matrix at each momentum $k\parallel$ and frequency, thus time consuming.

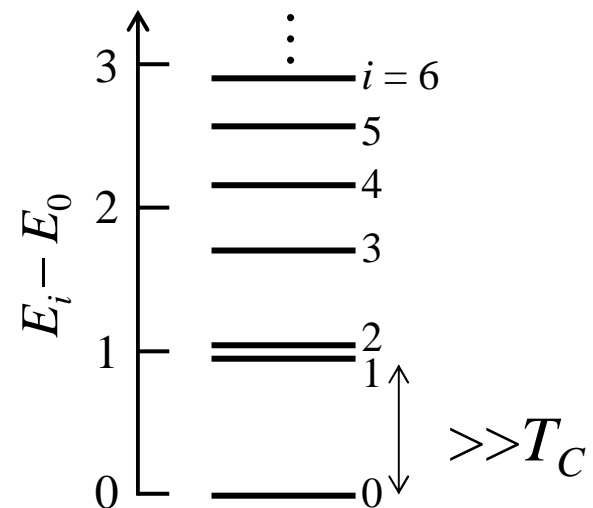
This talk: Only in-plane-symmetric phases

Trial: Magnetic phase diagram of single-band Hubbard model on an infinite-dimensional FCC lattice

QMC data: Ulmke, Eur. Phys. J. B **1**, 301 (1998).



Energy diagram
impurity part of 2-site DMFT
($U=4, n=0.5$)



Energy unit: variance of non-interacting DOS

Numerical methods with finite # of bath-orbital are
weak dealing with thermodynamics.

We want to do finite temperature calculation as well.

DMFT study 2: Magnetic ordering

Alternative: semiclassical approximation

Hasegawa, JPSJ **49**, 178; 963 (1980).
 S.O., Fuhrmann, Comanac, & A.J.M.,
 cond-mat/0502067.

Key point: $Un_{\uparrow}n_{\downarrow} = \frac{1}{4}U(\rho^2 - m^2)$

$$\begin{aligned}\rho &= n_{\uparrow} + n_{\downarrow} : \text{charge} \\ m &= n_{\uparrow} - n_{\downarrow} : \text{spin}\end{aligned}$$

Hubbard-Stratonovich transformation (complete square) against two terms:

$$\exp\left\{-\int_0^\beta d\tau Un_{\uparrow}(\tau)n_{\downarrow}(\tau)\right\} = \int D[\varphi, x] \exp\{-S_{int}\}$$

$$S_{int} = \frac{1}{4U} \int_0^\beta d\tau \left[\varphi^2(\tau) + x^2(\tau) - 2U \sum_{\sigma} c_{\sigma}^{\dagger}(\tau) \underbrace{\{\varphi(\tau)\sigma + ix(\tau)\}}_{\text{Spin-field}} c_{\sigma}(\tau) \underbrace{x(\tau)}_{\text{charge-field}} \right]$$

Semiclassical approximation:

keep φ ($i\nu_l=0$, zero Matsubara frequency) (spin field),

saddle-point approximation for x (charge field) at given φ .

↑ very slow spin-fluctuation dominates

$$G_{imp\ \sigma}(i\omega_n) = \int d\varphi e^{-V/T} [a_{\sigma}(i\omega_n) + (\varphi\sigma + i\bar{x})/2]^{-1}$$

$$\Sigma_{\sigma}(i\omega_n) = a_{\sigma}(i\omega_n) - G_{imp\ \sigma}^{-1}(i\omega_n)$$

↓

DMFT self-consistency equation

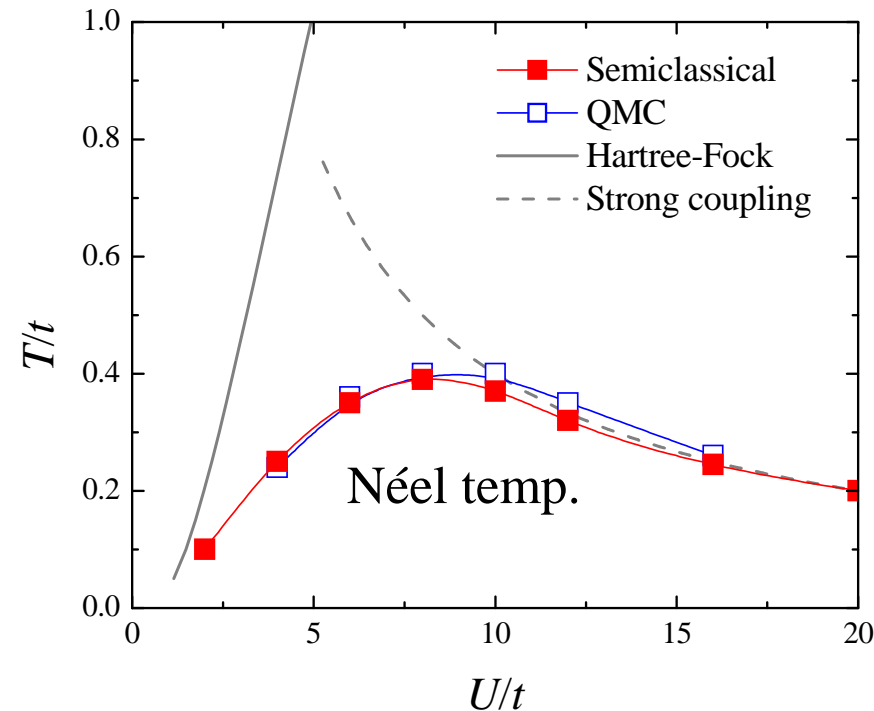
$$\left\{ \begin{array}{l} V = \frac{1}{4U} (\varphi^2 + \bar{x}^2) - T \text{Tr} \ln [-a_{\sigma}(i\omega_n) - (\varphi\sigma + i\bar{x})/2] \\ i\bar{x} = -UT \text{Tr} [a_{\sigma}(i\omega_n) + (\varphi\sigma + i\bar{x})/2]^{-1} \\ a_{\sigma}(i\omega_n): \text{Weiss field} \end{array} \right.$$

Examples of magnetic phase diagram by semiclassical DMFT

Hubbard model on various lattice

2D square lattice (half filling)

S.O., Fuhrmann, Comanac, & A.J.M.,
cond-mat/0502067.



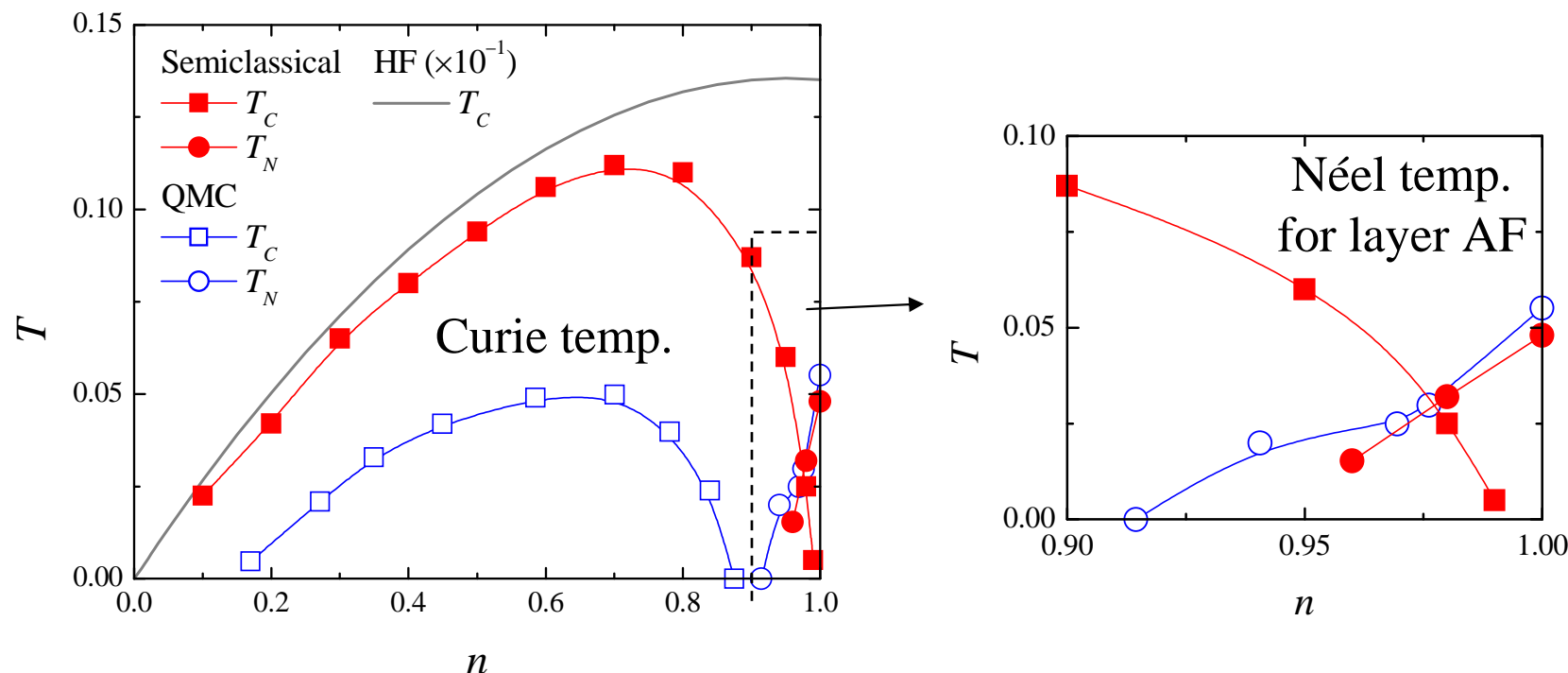
Semiclassical approximation gives excellent agreement with QMC.
 $n=1$: charge fluctuation is suppressed

Examples of magnetic phase diagram by semiclassical DMFT

3D face-centered-cubic (FCC) lattice

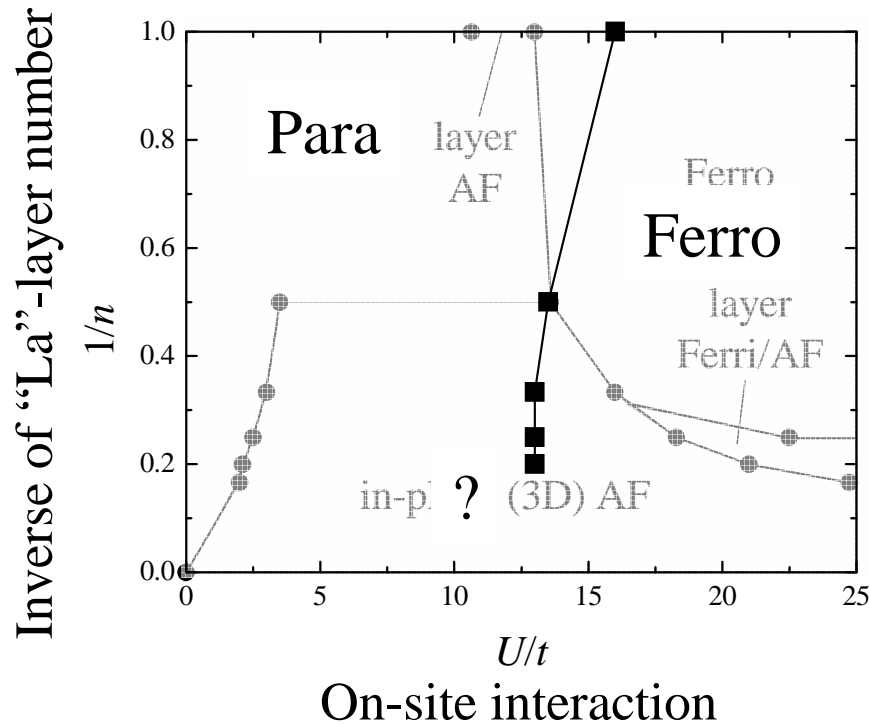
QMC data: Ulmke, Eur. Phys. J. B **1**, 301 (1998).

S.O., Fuhrmann, Comanac, & A.J.M.,
cond-mat/0502067.



T_c is higher than QMC by a factor ~ 2 ,
better agreement than HF and 2-site DMFT.
Correct n -dependence \Leftarrow Charge fluctuation
associated with spin fluctuation
Correct phase, AF phase at $n \sim 1$, is obtained.

Magnetic Phase Diagram DMFT result



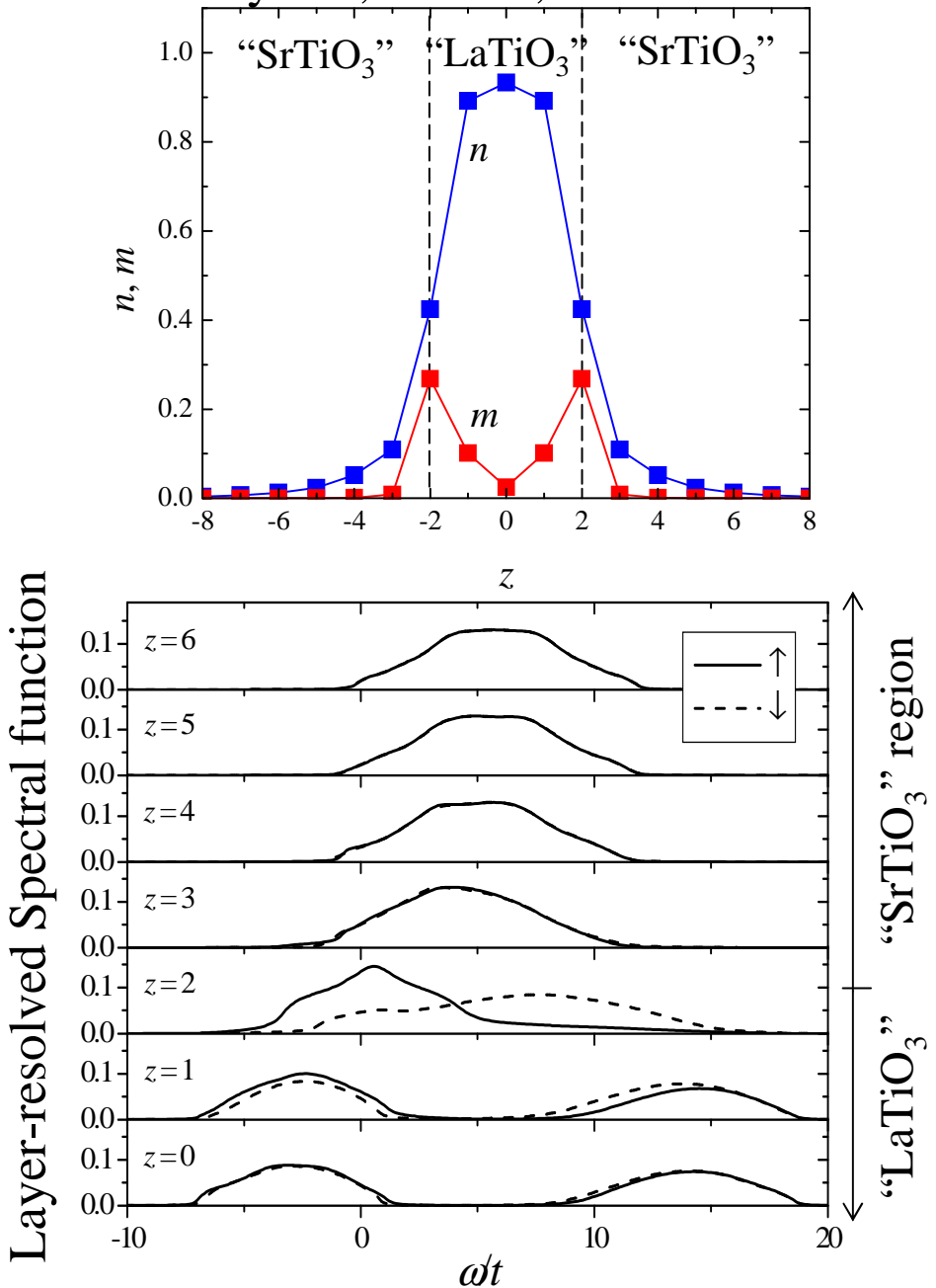
Layer Ferri/AF phases are washed away.

Ferromagnetic ordering appears at large U region, and prevails to large n .

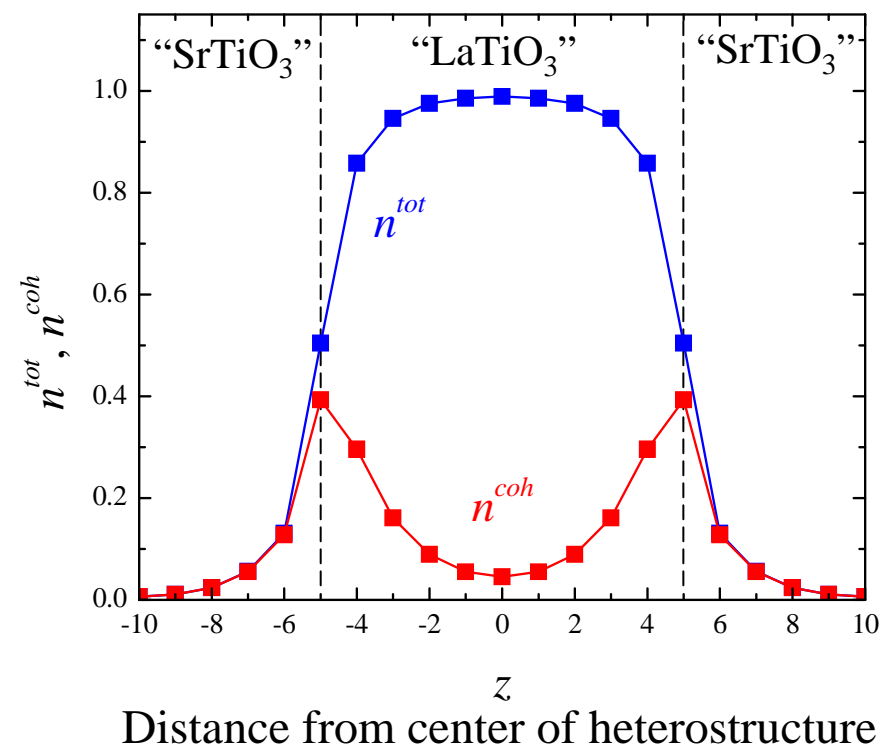
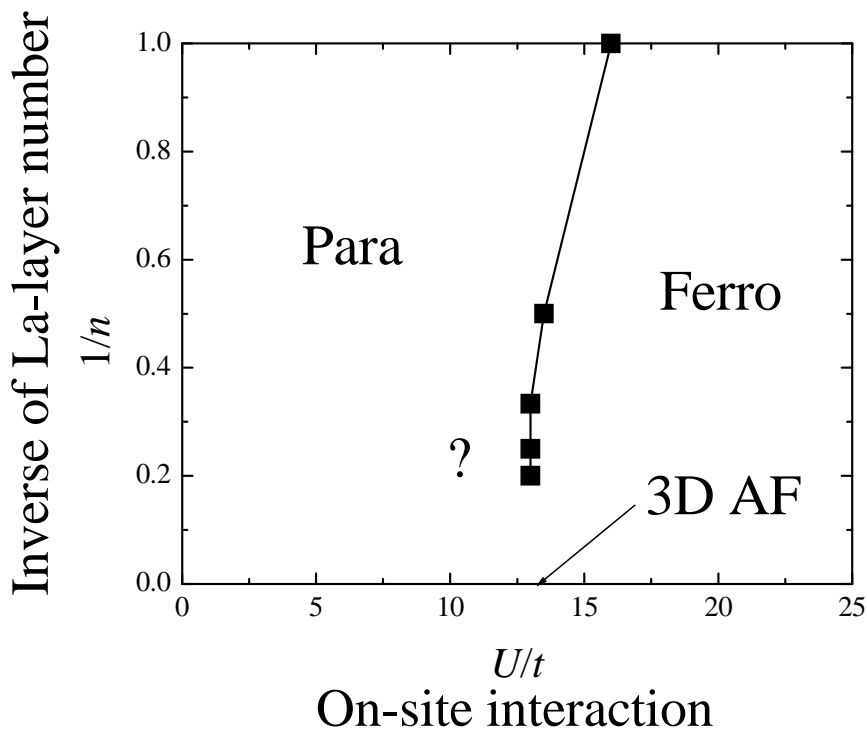
Magnetic moment appears at “interface region.”

In-plane symmetry breaking: now in progress.

“4 La-layers”, $U/t=18$, $T/t=0.1$



Main results of DMFT study on “1-orbital heterostructure”:
Different orderings in heterostructures than in the bulk
Metallic interface, ~ 3 unit cells wide.



Summary

Model calculation for $[\text{LaTiO}_3]_n/[\text{SrTiO}_3]_m$ -type heterostructure

Key word: “**Electronic reconstruction**”

Key results independent of details of theory:

Thin heterostructures show different orderings than in the bulk.

Interface region between Mott/band insulators (~3 unit cells wide) becomes always metallic.

Future problem

In-plane symmetry breaking: in progress

DMFT study on the realistic three-band model

How spin & orbital orderings are modified?

Combination between DMFT & 1st principle calculation

Effect of lattice distortion; largeness of ε , orbital stability

Material dependence

d^2, d^3, d^4, \dots systems, various combinations between them and with others